

Fig. 4.8 Velocity vectors on the cross plane $\theta = 0^\circ$ & 180° at steady state for $H = 20.0$ mm with $D_j = 10.0$ & 20.0 mm at $Ra = 0$ ($\Delta T = 0^\circ C$) for $Re_j =$ (a) 406 and 203 ($Q_j = 3.0$ slpm), (b) 541 and 270 ($Q_j = 4.0$ slpm), and (c) 676 and 338 ($Q_j = 5.0$ slpm).

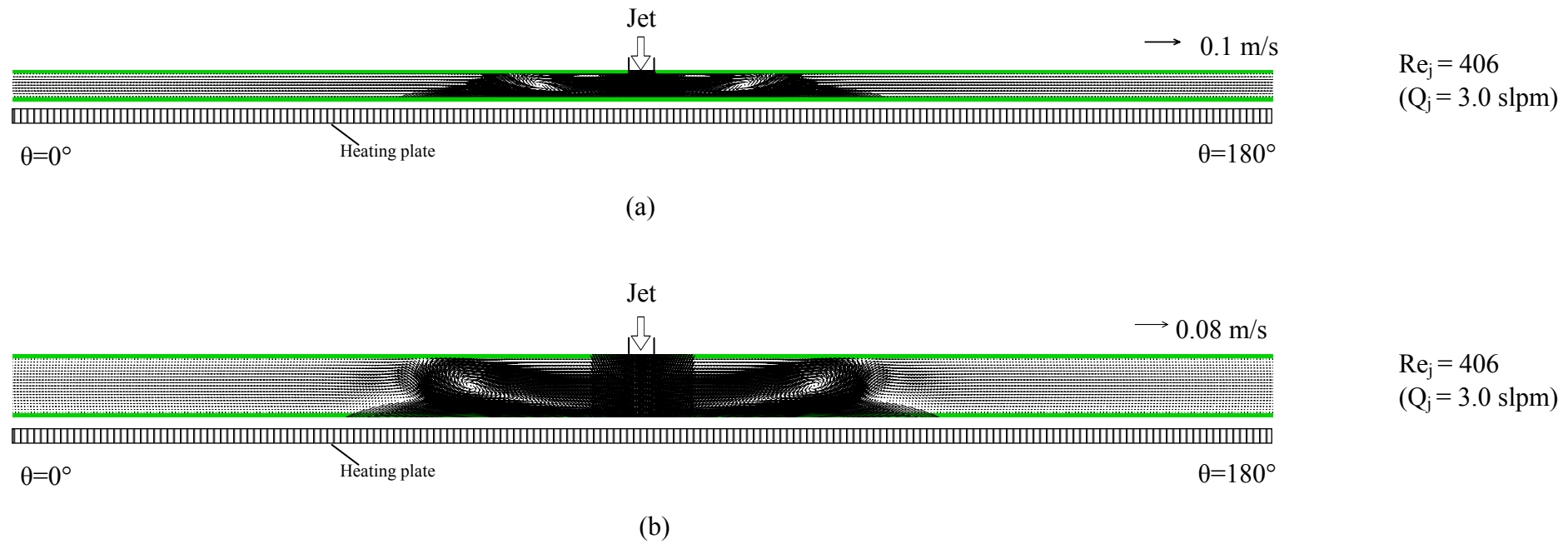


Fig. 4.9 Velocity vectors on the cross plane $\theta = 0^\circ$ & 180° at steady state for $D_j = 10.0 \text{ mm}$, $Re_j = 676$ ($Q_j = 5.0 \text{ slpm}$) at $Ra = 0$ ($\Delta T = 0^\circ\text{C}$) for $H =$ (a) 10.0 mm and (b) 20.0 mm .

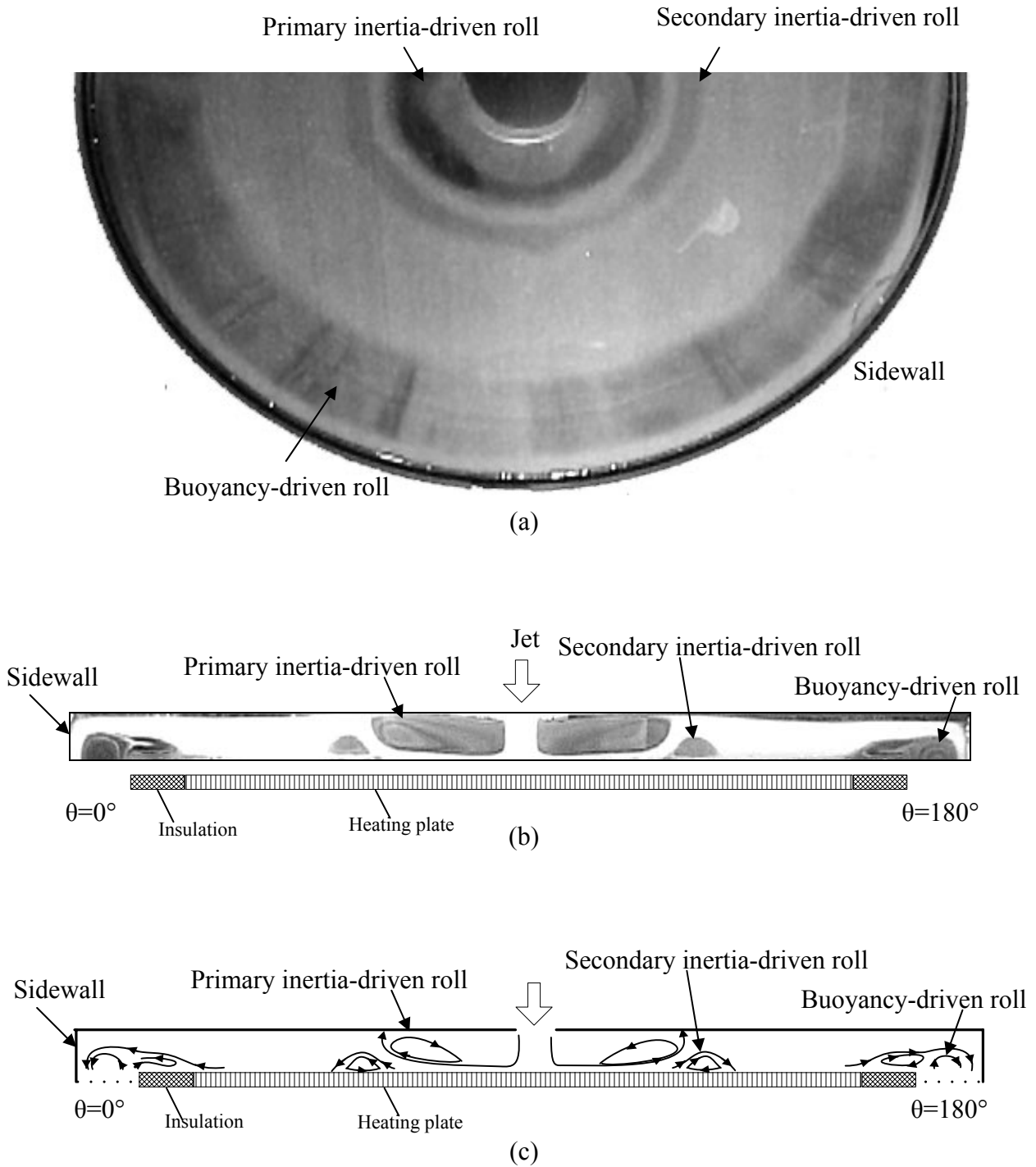


Fig. 4.10 Steady vortex flow pattern for $D_j=10.0$ mm and $H=15.0$ mm at $Re_j=406$ ($Q_j=3.0$ slpm) and $Ra=3,170$ ($\Delta T=10.0^\circ\text{C}$): (a) top view flow photo taken at the middle horizontal plane between the disk and chamber top, (b) side view flow photo taken at the vertical plane $\theta=0^\circ$ & 180° and (c) the corresponding schematically sketched cross plane vortex flow.

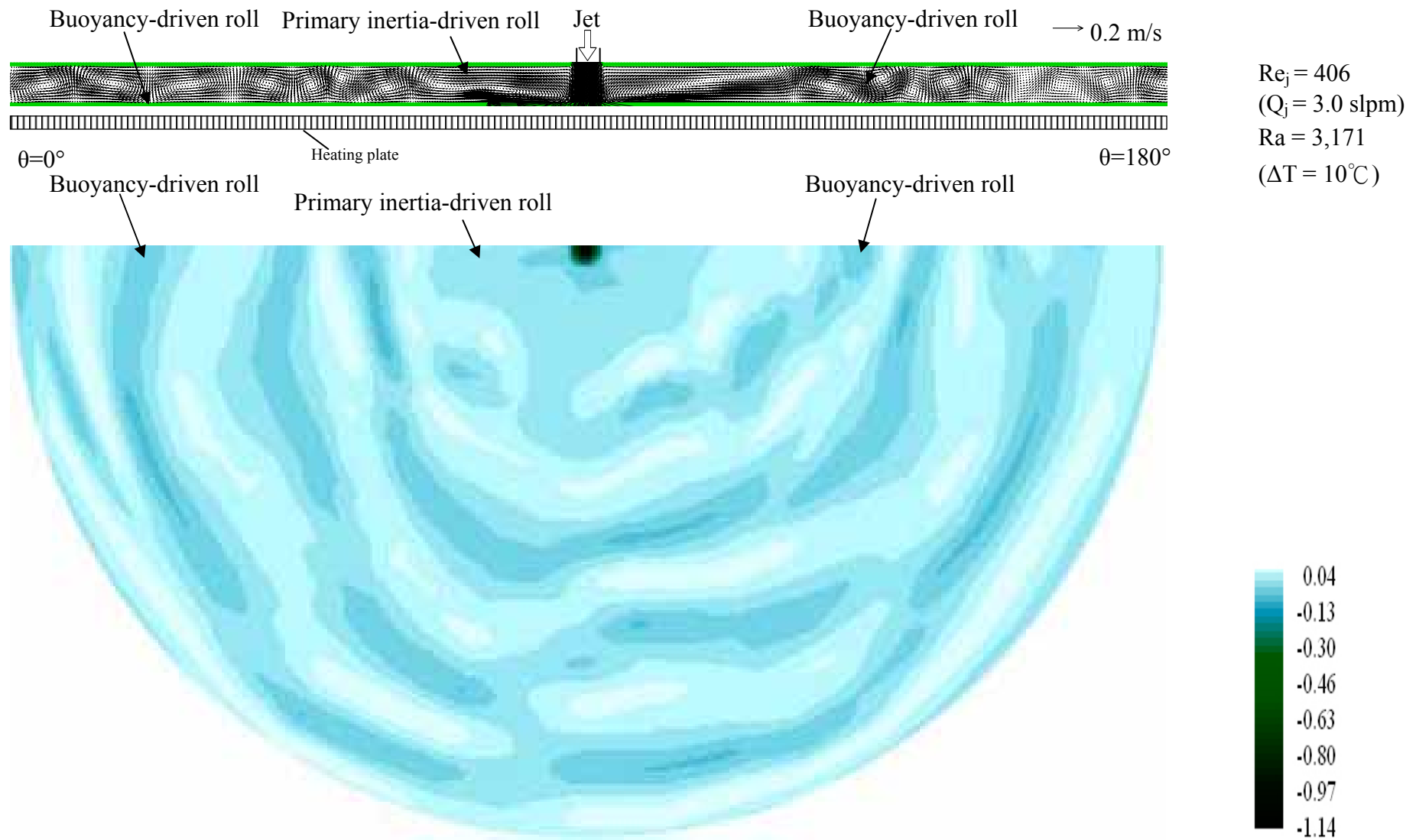


Fig. 4.11 Unsteady vortex flow at certain instant in statistical state for $H = 15.0 \text{ mm}$, and $Ra = 3,171$ ($\Delta T = 10^\circ\text{C}$) at $Re_j = 406$ ($Q_j = 3.0 \text{ slpm}$): (a) velocity vectors on the vertical plane $\theta = 0^\circ$ & 180° and (b) contours of the vertical velocity component w at the horizontal plane $z = -7.5 \text{ mm}$.

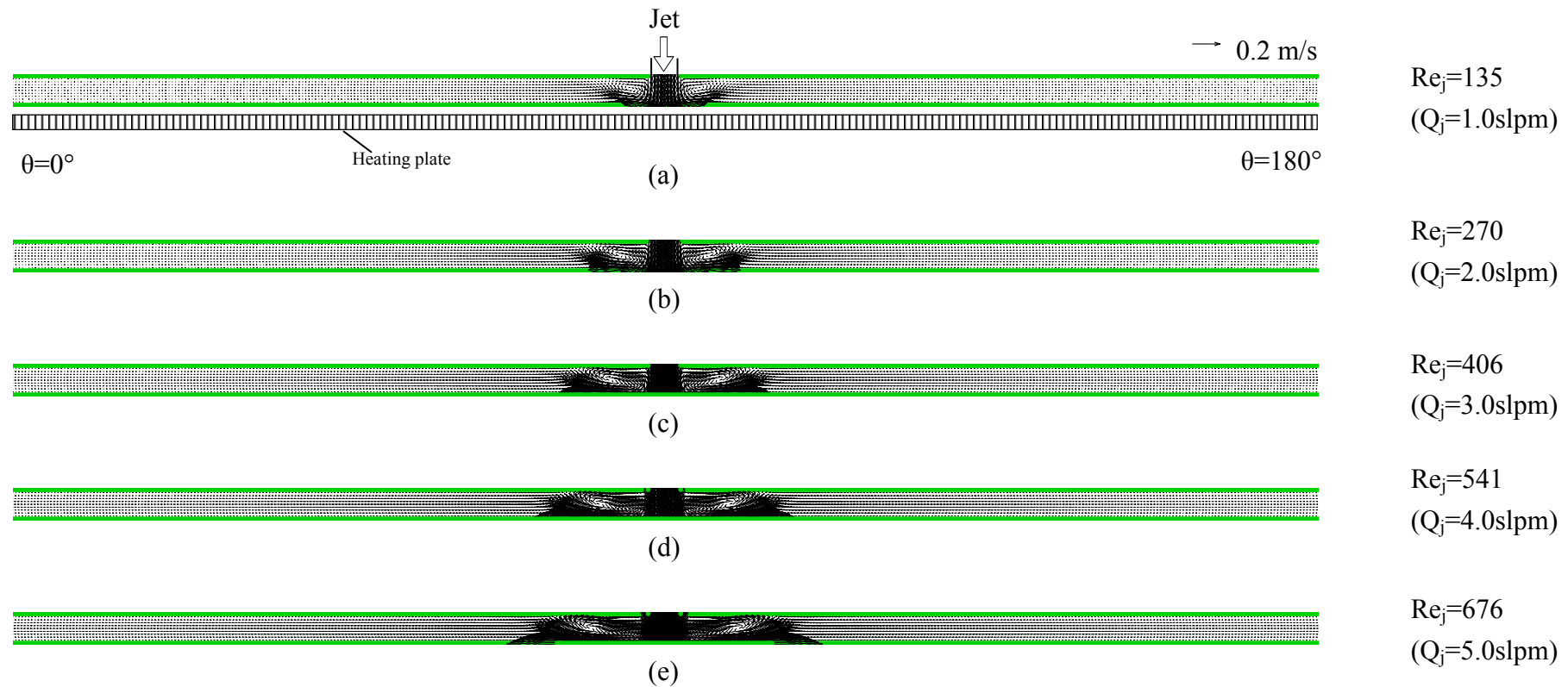


Fig. 4.12 Velocity vectors on the cross plane $\theta = 0^\circ$ & 180° at steady state for $D_j = 10.0$ mm, $H = 10.0$ mm, $Ra = 470$ ($\Delta T = 5^\circ\text{C}$) for $Re_j =$ (a) 135 ($Q_j=1.0$ slpm), (b) 270 ($Q_j=2.0$ slpm), (c) 406 ($Q_j=3.0$ slpm), (d) 541 ($Q_j=4.0$ slpm), and (e) 676 ($Q_j=5.0$ slpm).